Island analysis of low-activity dynamic speckles

Marcelo N. Guzmán,[1,2] G. Hernán Sendra,[3] Héctor J. Rabal,[2,*] and Marcelo Trivi[2]

[1]Laboratorio Laser, Facultad de Ingeniería, Universidad Nacional de Mar del Plata, Juan B. Justo 4302, CC 7600 Mar del Plata, Argentina

[2]Centro de Investigaciones Ópticas (CONICET La Plata—CIC) and UID Óptimo, Facultad de Ingeniería, Universidad Nacional de La Plata, P.O. Box 3, CC 1897 Gonnet, La Plata, Argentina

[3]Imaging Facility, Zentrum für Molekulare Biologie der Universität Heidelberg (ZMBH), Im Neuenheimer Feld 282, D-69120 Heidelberg, Germany

*Corresponding author: hrabal@ing.unlp.edu.ar

Received 30 August 2013; revised 22 November 2013; accepted 24 November 2013; posted 26 November 2013 (Doc. ID 196734); published 23 December 2013

In this work we present a method to evaluate activity in low dynamic speckle patterns. It consists of binarizing the speckle image and analyzing the displacements and deformations of the resulting speckle grain regions, here called *islands*. Numerical simulations and controlled experiments were used to study the variations of the island features with the aim of finding a correlation with the activity of the speckle pattern. From the obtained results it was possible to conclude that the developed method can be useful for the analysis of low activity speckle patterns with the advantage of requiring only pairs of frames, thus permitting the assessment of nonstationary processes. In the case of stationary phenomena, so that stacks of frames registers are representative of them, dilute activity images can also be constructed. © 2013 Optical Society of America

OCIS codes: (100.0100) Image processing; (120.0120) Instrumentation, measurement, and metrology; (030.6140) Speckle; (120.6165) Speckle interferometry, metrology.

http://dx.doi.org/10.1364/AO.53.000014

1. Introduction

When a surface is illuminated with a laser light it exhibits a granular diagram called speckle pattern due to pseudorandom interference phenomena. If the surface suffers any deformation or movement, this pattern fluctuates in time and is called dynamic speckle. Its dynamical properties are usually analyzed to infer properties of the sample that generates it. There are several techniques to evaluate the dynamics depending on the applications [1] so that it results in a useful tool for the nonintrusive and nondestructive analysis of some biological and industrial processes. Many applications using this technique were developed, but the detection and quantification of low activity is in some cases difficult to evaluate. Vortex analysis in a complex image was successfully employed before in optical metrology and has been found to achieve nanometric precision in some cases [2,3] using a similar approach.

In this work we present an approach for the temporal characterization of low activity speckle patterns by using geometrical characteristic parameters of the speckle grains (or islands). This new islands idea consists in analyzing the behavior of some features present in the grain of speckles. Each grain in a speckle image has some attributes that, when varying in time, can be used to characterize the local activity of the pattern. Nevertheless, in dynamic processes, grains or islands are both created and annihilated, and thus the process of finding the homologous ones in consecutive frames is inherently not warranted, as it is also the case with optical vortices.

This method also requires only pairs of frames, but it is simpler than the vortex analysis. The computational cost is lower because no mathematical transformation is required.

1559-128X/14/010014-08$15.00/0

The application of this method begins with the binarization of the speckle image using a threshold that defines some grain regions called islands. These islands can be characterized in terms of area, perimeter, eccentricity, mass center, etc. [4]. We analyze then the time behavior of these parameters in order to find a correlation with the pattern activity. The method was evaluated with patterns generated by rigid body displacement under the following situations: pure translation, pure boiling, and mixed translational-boiling resulting speckle patterns [5]. We used both numerical simulations and controlled experiments to generate dynamic speckle patterns with different activity levels [6,7]. A moving diffuser with different velocities was employed to generate several activity levels. Two optical setups were also tested: free propagation and image formation.

We present here several simulations and controlled experimental results oriented to evaluate the advantages and limitations of the proposed technique. In each example, we analyze the correlation between the studied parameters and the diffuser velocity. The percentage of correctly identified homologous islands is also shown and Brownian motion compensation was included to linearize the results [7].

Finally, the possibility of construction of activity images showing loci of equal activity, though requiring more frames, is commented upon.

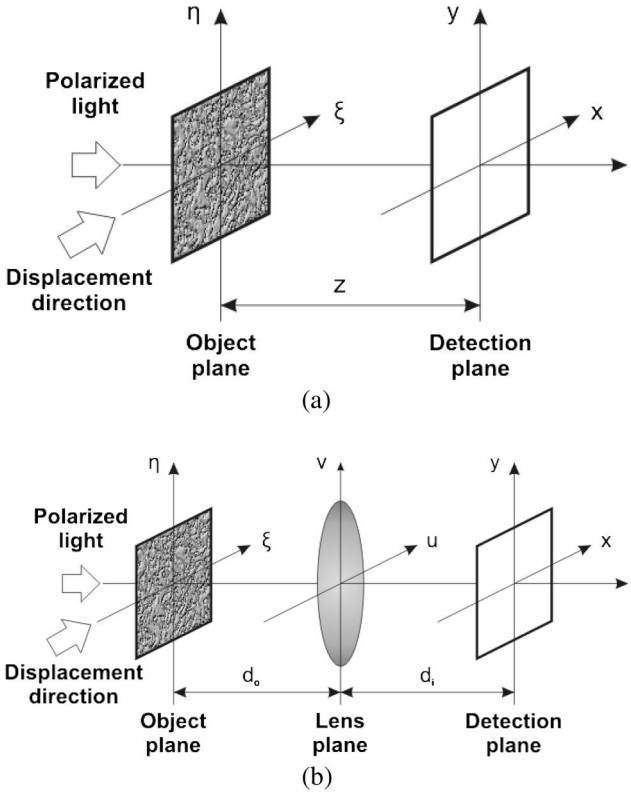

Fig. 1. Set-up employed to generate the speckle patterns: (a) Free-space propagation geometry and (b) propagation through a lens (focused or defocused).

2. Theory

A. Translational and Boiling Speckle Patterns

Boiling speckle patterns appear in several situations involving both biologic and industrial specimens. Characterization is very difficult because of the huge number of variables that are hard to monitor. So, in this work we have used a similar approach as that in the case of vortices, i.e., simulated and experimental controlled dynamic patterns obtained from the displacement of a diffuser [7]. Two geometrical situations were evaluated: The first one is a free-space propagation scheme or objective speckle [Fig. 1(a)], while the other one uses a lens to get focused and defocused subjective speckles images [Fig. 1(b)].

When the diffuser is moved in its plane, the observed speckle becomes a dynamic pattern that may or may not replicate the movement of the object. If each speckle grain reproduces the object movement, the speckle is called translational speckle. On the other hand, if no object movement can be inferred from the dynamic speckle, i.e., if the intensity distribution fluctuates in a seemingly random way in time, then the speckle pattern is called boiling speckle [1]. Between those extremes, there exists a continuum where the grains both displace and boil in different proportions.

B. Pure Translation and Pure Boiling

In the most general situation, both phenomena occur simultaneously. However there exist some conditions where it is possible to observe pure translational or pure boiling speckle patterns. Okamoto and Asakura [5] describe these conditions using the normalized spatiotemporal autocorrelation function. When the velocity of this function is zero, we observe a pure boiling speckle pattern.

For free-space propagation geometry [Fig. 1(a)], the condition is

$$1+\frac{z}{\rho}=0, \tag{1}$$

and for propagation through a lens [Fig. 1(b)], the condition is

$$\left(\frac{1}{d_O}+\frac{1}{d_i}-\frac{1}{f}\right)\left(1+\frac{d_O}{\rho}\right)-\frac{1}{d_O}=0. \tag{2}$$

In both cases, ρ is the wavefront curvature radius of the light incident on the moving diffuser.

On the other hand, a pure translational phenomena can only be observed using a lens and when the curvature of the wavefront is equal to minus the object distance ($\rho=-d_o$).

(In actual experimental conditions, a certain amount of boiling speckle cannot be avoided.) In this way, the conditions determined by Okamoto and Asakura provide a controlled way to generate boiling speckle that can be experimentally repeated and

reproduced without the inherent variability of, for example, biologic phenomena.

In this work we analyze pure boiling and pure translational speckle patterns that are both obtained using the scheme shown in Fig. 1(b).

In the first case we chose $d_o = d_i = f = 50$ cm and $\rho = \infty$ (plane-wavefront). We used object and lens pupils with a diameter of 6 mm and 1 cm, respectively.

For the case of pure translational speckle, we used $d_o = 33.3$ cm, $d_i = 1$ m, $\rho = -d_o$, an object pupil diameter of 6 mm and a lens pupil of 1 cm.

Both geometries were studied before [6,7] using both a numerical model and an actual experiment, exhibiting very similar results.

3. Methods

A. Islands Analysis

We propose an approach to study low-activity speckle patterns that consists of analyzing the attributes of the binarized speckle grains. The process has the following stages: (1) binarization of the speckle image, (2) characterization of the speckle grains (islands) by measuring its attributes, (3) identification of homologous islands in consecutive frames, and (4) measurement of displacement or changes in other properties between the already found homologous islands.

1. *Binarization*

The digitalization of the speckle grain produces an image where its elements are integer numbers proportional to the registered intensity, in our case in the range 0–255. The binarization consists in applying a threshold u_b to each pixel of the image that assigns a value of 0 if the pixel intensity is less than u_b and 1 if it is higher [4]. This threshold is empirically chosen and depends on the intensity histogram and noise level of the original image. A sample speckle pattern and its binarization are shown in Figs. 2(a) and 2(b), respectively. Each binarized speckle grain will be denoted as an *island*.

2. *Island Characterization*

The islands present in the binarized image [Fig. 2(b)] have several geometrical features that allow their characterization in order to identify the correspondence between grains in consecutive frames. In this work we calculate their mass center position, area, perimeter, and the ellipse that better approximate the shape by the least-squares method (Fig. 3). Therefore, each island is characterized by its area and perimeter, as well as the eccentricity and inclination of the corresponding ellipse [4].

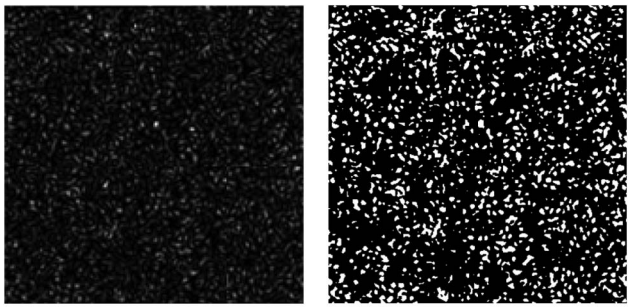

(a) (b)

Fig. 2. (a) Speckle pattern and (b) resulting image after binarization.

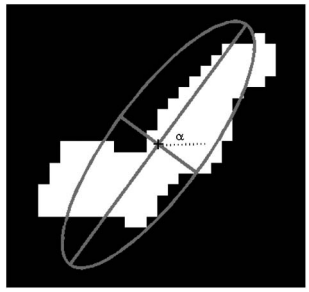

Fig. 3. Sample thresholded speckle grain (island) and its corresponding best fitting ellipse, where the mass center and the angle of inclination α can be appreciated.

3. *Identification of Homologous Islands*

For the detection of homologous islands, a set of threshold conditions is applied to the variations of one or more properties, leading in this way to a reduced list of candidates. Since we are dealing with boiling patterns where the speckle grains suffer a continuous deformation, only one threshold on the maximum Euclidean distance was used.

After that, a merit function J is then applied to all the surviving islands, defined as

$$J = \Delta\varepsilon^2 + \left(\frac{A - A'}{A + A'}\right)^2 + \left(\frac{2}{\pi}\Delta\alpha\right)^2, \tag{3}$$

where A is the island area, ε the eccentricity of its best fitting ellipse, and α the angle of its major axis with respect to an arbitrarily chosen direction. Primes indicate the same parameters tested for correspondence in one of the following frame islands. The J parameter acts as a merit function assigned to each island pair. A threshold is also used here to eliminate candidates in the neighborhood that are completely different. The final homologous island is the one with minimum merit function.

4. Experiments

In order to test the method in controlled and reproducible conditions, we used the same optical setup described in [7], whose geometrical schemes are outlined in Fig. 1, where the object plane consisted of a ground glass diffuser. We used a polarized light coming from the He–Ne laser Melles Griot 10 mW power. The diffuser was displaced using an Aerotech ARS 302 MM stepping motor (2 μm per step). Images were recorded by a CCD Pulnix TM 6CN camera (pixel size 8.6 μm × 8.3 μm), connected to a personal

computer with a frame grabber and digitized to 256 intensity levels (8 bits).

Regarding the geometry for pure translation, a small amount of boiling is unavoidable in experimental conditions. The conditions and geometrical experimental parameters for translational speckle patterns with boiling and for pure boiling speckle patterns were reproduced from the work of Sendra *et al.* [6].

5. Simulations

A numerical model was also used to generate simulated boiling speckle patterns according the schemes of Fig. 1, where a random matrix acted as the diffuser scattering centers. We empirically adjusted the optical matrix and the discretization parameters to obtain a well-developed speckle grain of 5 to 6 pixels size per grain. The simulation of a rigid diffuser in movement was achieved by shifting the diffuser phase matrix. The mathematical expressions to propagate the optical field from the diffuser U_o to the observation plane U_d were analyzed by Goodman [8] and numerically simulated by Sendra *et al.* [6]. The planes where discretized using a square grid, using a carefully chosen spatial sampling period to fulfill the sampling theorem and avoid subsampling effects.

To generate the rotational speckle pattern, the "in rotate" MATLAB function was used. This function takes a frame and rotates it an angle, 10° in this case, in a counterclockwise direction around its center point.

6. Results

After the simulation of consecutive frames or the acquisition of images in actual experiments and the subsequent identification of corresponding speckle islands, the Euclidean distance was calculated between the mass centers of the islands for both almost pure translation and pure boiling situations.

Figure 4 shows the results of the islands method for speckle translation with small boiling in (a) simulation and (b) controlled experiment. A very good agreement can be appreciated between the actual diffuser displacement and average islands displacements, in both cases with a Pearson squared coefficient $r^2 = 0.99891$ and $r^2 = 0.99553$, respectively. In actual experiment, it can be seen that error bars increase for larger displacement due to the boiling speckle. The measurements are linear up to about 100 μm, which is a reasonable limit for speckle methods.

In order to determine the minimum amount of movements that can be detected, we explored the subpixel measurement capability of the island approach. A large moving diffuser object was used to simulate 10 frames of 1000 × 1000 pixels. Each frame corresponded to a step of one single pixel in the translation of the diffuser. A "binning" operation was applied to each frame, which consists in applying a grid with a period of 10 × 10 pixels and then converting each grid cell in a single pixel whose value is the average of the 10 × 10 pixels. As a result, a new set of 10 frames with 100 × 100 pixels was generated, where each frame corresponds to a translation of 1/10 pixels. Figure 5 shows the results for subpixel simulation. Very good agreement can be seen with $r^2 = 0.99384$. The measurement errors are caused by averaging the frames. So, the pure translation is transformed into a pure translation with boiling.

To test the effects of noise on the islands method, Gaussian white noise was added on a pure translational speckle example. A displacement of 3 μm on the x axis and 0 μm on the y axis was simulated between two consecutive frames. Then, Gaussian white noise was added with zero mean and a variance whose values were increased from 0.1 to 10.1 in 0.2 steps. Figure 6 shows the results. We assume that the noise effects become important for a variance greater than 6.

As in the translation case, an experimental rotation with no boiling cannot be obtained in coherent light illumination. A small amount is always present. In order to test the method in the situation of rotation, a simulation of pure translation was used.

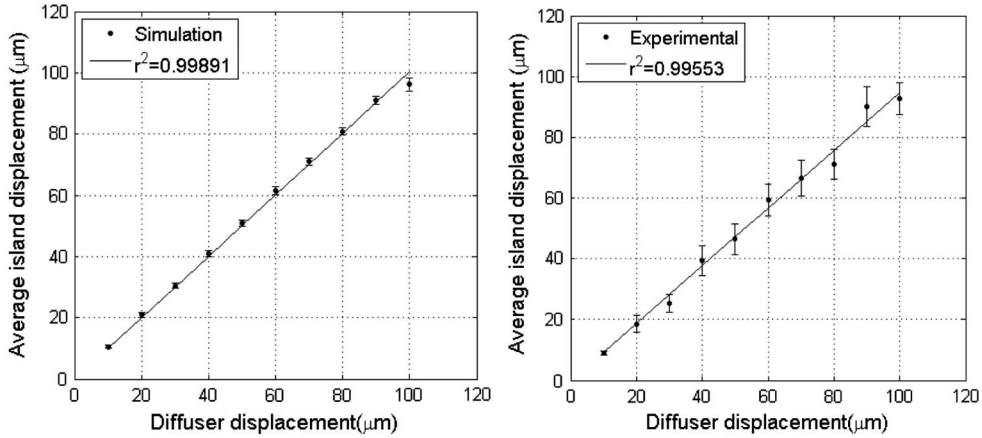

Fig. 4. Result of the application of the islands method for speckle translation with boiling displacements in (a) simulation and (b) controlled experiment. Figures show the average island displacement versus the diffuser displacement.

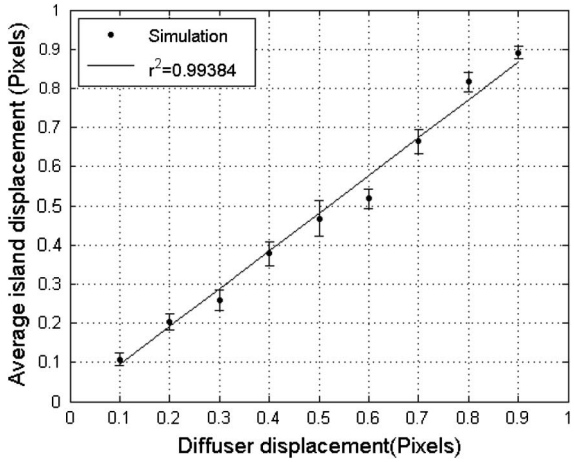

Fig. 5. Average island displacement for subpixel simulated diffuser displacement, in pure translation condition.

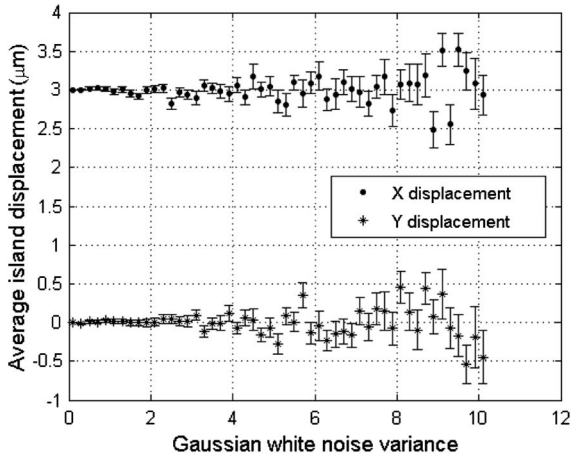

Fig. 6. Effect of Gaussian white noise variance on the translation of the islands, in pure translational condition.

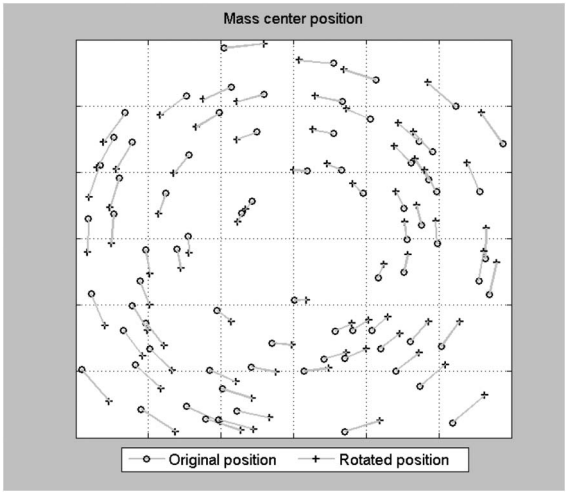

Fig. 7. Island method applied to a simulated (pure translation) in-plane rotational measurement with a rotation of 10° between initial (circle) and final (cross) positions.

Figure 7 shows an in-plane rotational measurement with a rotation of 10° between the initial (circle) and final (cross) mass center position of homologous islands. For larger rotations, there is a decrease in the number of homologous islands that can be correctly identified. It is noteworthy to mention that in this case, the external displacements are higher than the 100 μm.

For pure boiling examples, Figure 8 shows (a) the Euclidean distance between the identified islands and (b) the proportion of identified islands.

The displacements of the islands, in both numerically simulated and experimentally obtained situations, show a nearly linear and reasonable agreement for low displacements (50 micrometers or less) and depart from linearity and agreement at larger displacements or the corresponding velocities. As can be expected, when the displacements are larger, the proportion of well identified islands decreases mainly due to decorrelation resulting in higher measurements errors.

The islands displacements exhibit thus a similar behavior to the vortices displacements (see [7]) although with increased noise. Noisy results were also found in the experimental boiling pattern. The number of identified islands is considerably higher compared with the identified vortices in identical conditions.

The processing time of speckle islands and vortices methods for a typical measurement of displacement between two consecutive images is only 1.5 seconds.

A. Correction for Brownian Motion

If we consider that the islands displacements in pure boiling simulations have random directions, we can treat their movement as a Brownian motion [7,9]. A feature of plane Brownian motion (as a random walk) is that the total averaged displacement d_T after N_l time intervals of displacements of length l is

$$d_T = l\sqrt{N_l}. \tag{4}$$

The value of l is not known, but it is directly proportional to the averaged Euclidean distance. Hence if we plot the product of the averaged Euclidean distance times the square root of the diffuser velocity versus the diffuser velocity, we should obtain a straight line. This is evidenced in Fig. 9(a), where, for the smaller displacements 75 μm/frame appears a linear zone where "*islands*" can be considered to exhibit a Brownian behavior. A linear regression in that range results in the model $y = 0.9367$ x, with a Pearson squared coefficient $r^2 = 0.9945$.

Finally, to set the resolution in the measurement of displacement, the largest error was used to define a confidence interval. The estimated resolution in the measure of the diffuser displacement was 5.37 μm. It is important to note that the range for the displacements was from 0 to 75 μm (low activity region) in order to make a fair comparison with the vortices. If the same procedure is performed for smaller

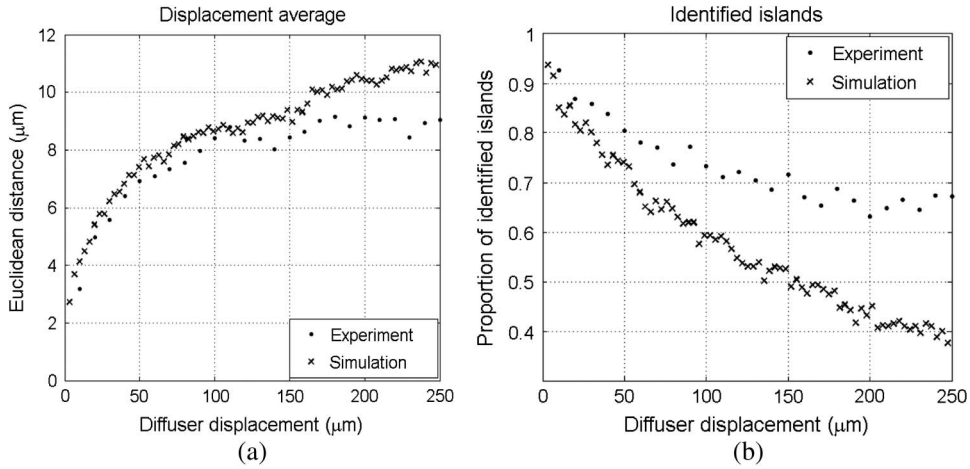

Fig. 8. (a) Averaged Euclidean distance of the islands displacements in pure boiling speckle for simulation (crosses) and experiment (dots) and (b) the corresponding number of identified islands.

movements, resolution improves, as well as the correlation coefficient of the estimation. The linearity of the *islands* movements in the defined area and the linear regression can be appreciated in Fig. 9(b).

B. Activity Images

After finding the preceding results that indicate that speckle activity can be estimated by using the islands approach, we intended to use it for the construction of equal activity images.

Images of the loci of equal island displacement can also be constructed. In order to test this possibility, we simulated an image with two different displacements by pasting halves of the images used in the described measurements of displacements, considering the result as a composite image. This is a raw approach to the historical experiment of Burch and Tokarsky [10] in early speckle metrology using photographic registers.

Then the local displacement of each island was measured and the corresponding positions plotted before and after the displacement, as is shown in Fig. 10. Notice that in the bottom of Figs. 10(a) and 10(b), the displacement increases more than in the top.

With the results obtained before for the local displacements, we built an image by assigning a proportional intensity to each pixel depending on the displacement value. This image can be seen in Fig. 11(a). As the identified islands are sparse, we blurred this result to improve its visual appearance, as is shown in Fig. 11(b). Even though the identified islands are sparse, the regions with different displacements can be clearly identified.

The same procedure was also tested with a set of dynamic speckle images obtained from a biological sample (as in [11]).

A Petri dish containing motile bacteria (*Pseudomona aeruginosa*) and a fungus were illuminated by a laser through a diffuse screen and a set of images were recorded by a CCD camera and processed to find local islands displacements. A new image was constructed with intensity levels proportional to the measured displacements and false color was assigned (Fig. 12). Results are in qualitative agreement with those found in a previous work (for details

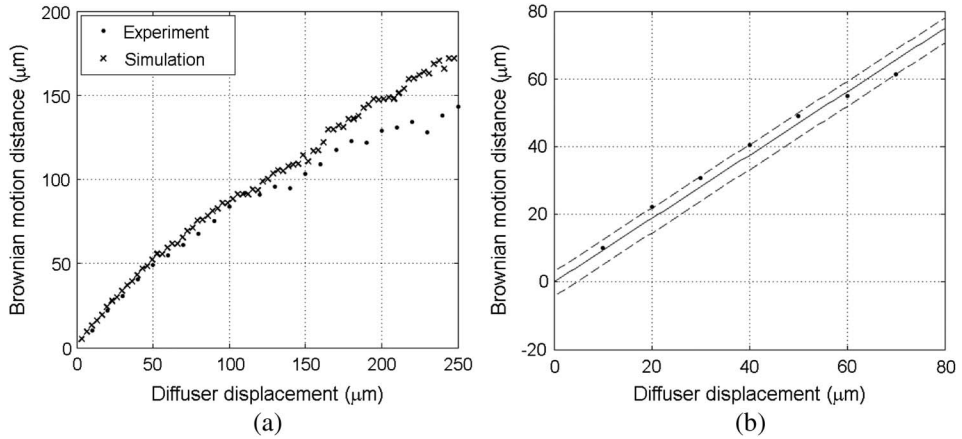

Fig. 9. (a) Product of the average Euclidean distance of displacement of the "islands" times the square root of the diffuser displacement versus the displacement of the diffuser. The graph (b) is an enlargement of (a) considering only experimental data. A linear regression was applied, and the dash lines shows the maximum deviation of the samples from the regression line.

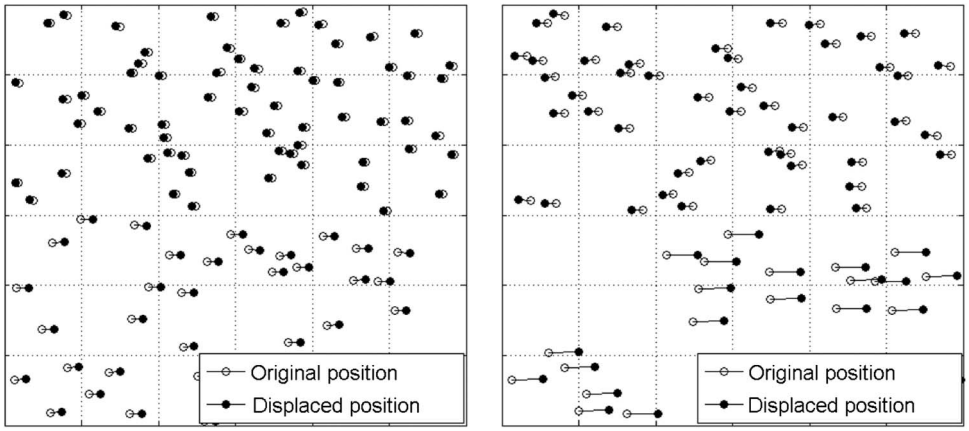

(a) (b)

Fig. 10. Displacements measurements. Upper and lower halves of the figures were horizontally displaced in different amounts and opposite directions: (a) 10 and 20 μm and (b) 10 and 80 μm, respectively.

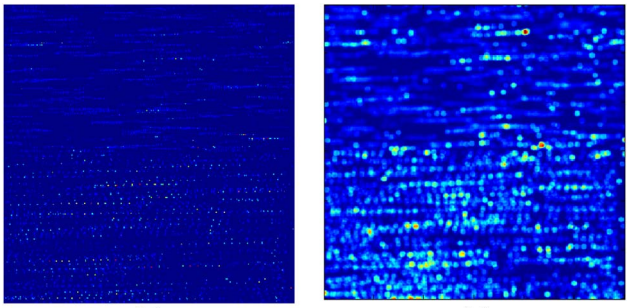

(a) (b)

Fig. 11. (a) Displacements of the islands shown as intensity levels. (b) Gaussian blurred version of (a).

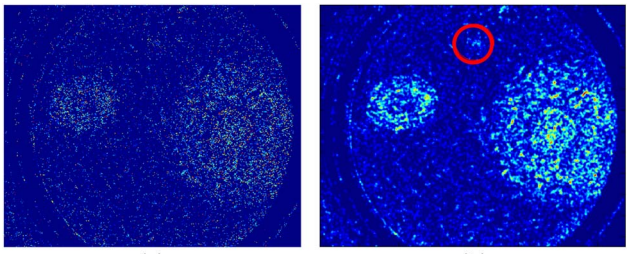

(a) (b)

Fig. 12. Application of activity images in a Petri dish with two colonies of bacteria and a fungus: (a) Image obtained with the islands and (b) its Gaussian blurred version. The fungus exhibits lower activity (inside a red circle).

and comparison see [11]). The region occupied by bacteria can be distinguished, as well as the fungus but with a considerable lower activity (see inside the red circle).

As the identified islands density is low, the images are very diluted. However, a very low activity sample, as it is the presence of a fungus (inside the red circle in Fig. 9), can be perceived.

7. Conclusions

The analysis of low-activity speckle patterns presents several problems for characterizing activity levels, either qualitatively or quantitatively, since there are not many descriptors with the necessary sensitivity and resolution. In this work we described the spatiotemporal analysis of low activity speckle patterns by means of studying the dynamic of their speckle grains (islands).

We have shown numerical and experimental evidence that dynamic speckle activity, for low values or for high temporal sampling rates, can be estimated from the mean displacement of the mass center of the islands. A very similar procedure as that used in vortices was also detection, characterization, and tracking. We performed experimental and simulations measurements using the islands method for both translation and pure boiling situations. We have also found that islands show Brownian motion behavior in pure boiling speckle patterns. In pure boiling experiments, the Euclidean displacements of the islands, corrected by Brownian motion, are proportional to the diffuser displacement and thus also well approximated to the speckle activity. Also, we found remarkable results for simulation and experiment in the translation case.

These results suggest that this approach would be a suitable tool for the evaluation of low level activity, especially considering the good agreement (linearity and precision) of the low activity region with high regression coefficients found in the controlled experiments and simulations shown in Section 6. The maximum islands displacements as well as the possibility of sub-pixel detection, the influence of the noise, the general accuracy, and errors were also analyzed.

One of the most important advantages of the presented method is that the results can be obtained requiring only two consecutive frames (with the exception of the activity images), in contrast with some other known methods [1] that require stacks of several images. So, activity in nonstationary phenomena could be followed. Besides it is conceptually very simple and no complex transforms are required as when using vortices. The vortices method usually requires additional calculations because it employs a

Laguerre–Gauss (or similar) transformation. Also the island method requires less memory for operations, reducing the computational cost, which can facilitate an eventual implementation for measurements in real time. The misidentification of homologous islands, as in the case of vortices, introduces errors in the measurements. Speckles suffering translation with boiling not only translate but also change shape. So, identification of homologous islands is increasingly more difficult as boiling increases. In the general case, the movement consists of a superposition of boiling and mechanical translation. It is of importance to measure both effects separately. As is the case with vortices, if the translation is as a rigid body, the mean value of the whole translation can be estimated and subtracted to obtain a pure (but modified) boiling condition. But an accurate determination of the rigid body movement requires homologous grains to be correctly assigned. This difficulty is being treated and will be reported in the future.

Even if the proportion of identified islands results in low resolution and diluted images, activity images of low activity samples can be constructed using this approach. This result suggests that also activity images (although diluted) could be built by using vortices or by combining both techniques.

We are now studying methods to improve the identification processes in order to reduce errors and extend the applicability for higher activities and better resolution in the activity images.

This method could be of use for the characterization of slow dynamic speckle phenomena, such as corrosion or efflorescence. As these experiments use the mechanical motion of a diffuser, they can be easily reproduced in comparison to biological phenomena and could be a first step to propose a standard for dynamic speckle measurements.

This work was supported by Consejo Nacional de Investigaciones Científicas y Técnicas (CONICET) PIP No. 112-201101-00520, Agencia Nacional Promoción Científica y Tecnológica (ANPCyT), PICT 2008/1430, Comisión de Investigaciones Científicas de la Provincia de Buenos Aires (CICPBA), Universities of La Plata (Grant 11/I150), and Mar del Plata, Argentina.

References

1. H. J. Rabal and R. A. Braga, Jr., eds. *Dynamic Laser Speckle and Applications* (CRC Press, 2008).
2. W. Wang, T. Yokozeki, R. Ishijima, A. Wada, S. G. Hanson, Y. Miyamoto, and M. Takeda, "Optical vortex metrology for nanometric speckle displacement measurement," Opt. Express **14**, 120–127 (2006).
3. W. Wang, T. Yokozeki, R. Ishijima, M. Takeda, and S. Hanson, "Optical vortex metrology based on the core structures of phase singularities in Laguerre-Gauss transform of a speckle pattern," Opt. Express **14**, 10195–10206 (2006).
4. K. R. Castleman, *Digital Image Processing* (Prentice Hall, 1996).
5. T. Okamoto and T. Asakura, "The statistics of dynamic speckles," in *Progress in Optics*, E. Wolf, ed., Vol. **34** (North Holland, 1995).
6. G. H. Sendra, H. Rabal, M. Trivi, and R. Arizaga, "Numerical model for simulation of dynamic speckle reference patterns," Opt. Commun. **282**, 3693–3700 (2009).
7. G. H. Sendra, H. Rabal, R. Arizaga, and M. Trivi, "Vortex analysis in dynamic speckle images," J. Opt. Soc. Am. A **26**, 2634–2639 (2009).
8. J. W. Goodman, *Introduction to Fourier Optics*, 2nd ed. (McGraw-Hill, 1996).
9. B. D. Hughes, *Random Walks and Random Environments*, Vol. **1** (Clarendon, 1995).
10. J. M. Burch and J. Tokarski, "Production of multiple beam fringes from photographic scatterers ," Opt. Acta **15**, 101 (1968).
11. S. Murialdo, L. Passoni, M. Guzman, G. Sendra, H. Rabal, M. Trivi, and J. Gonzalez, "Discrimination of motile bacteria from filamentous fungi using dynamic speckle," J. Biomed. Opt. **17**, 056011 (2012).